JCTC Journal of Chemical Theory and Computation

Article

pubs.acs.org/JCTC

Performance of an Optimally Tuned Range-Separated Hybrid Functional for 0−0 Electronic Excitation Energies

Denis Jacquemin,*[,†,‡] Barry Moore, II,[§] Aurélien Planchat,[†] Carlo Adamo,[⊥,‡] and Jochen Autschbach*[,§]

[†]Laboratoire CEISAM−UMR CNRS 6230, Université de Nantes, 2 Rue de la Houssinière, BP 92208, 44322 Nantes Cedex 3, France

[‡]Institut Universitaire de France, 103, bd Saint-Michel, F-75005 Paris Cedex 05, France

[§]Department of Chemistry, University at Buffalo, State University of New York, Buffalo, New York 14260-3000, United States

[⊥]Laboratoire LECIME−UMR CNRS 7575, Chimie-ParisTech, 11 rue P. et M. Curie, F-75231 Paris Cedex 05, France

Supporting Information

ABSTRACT: Using a set of 40 conjugated molecules, we assess the performance of an "optimally tuned" range-separated hybrid functional in reproducing the experimental 0−0 energies. The selected protocol accounts for the impact of solvation using a corrected linear-response continuum approach and vibrational corrections through calculations of the zero-point energies of both ground and excited-states and provides basis set converged data thanks to the systematic use of diffuse-containing atomic basis sets at all computational steps. It turns out that an optimally tuned long-range corrected hybrid form of the Perdew−Burke−Ernzerhof functional, LC-PBE*, delivers both the smallest mean absolute error (0.20 eV) and standard deviation (0.15 eV) of all tested approaches, while the obtained correlation (0.93) is large but remains slightly smaller than its M06-2X counterpart (0.95). In addition, the efficiency of two other recently developed exchange-correlation functionals, namely SOGGA11-X and ωB97X-D, has been determined in order to allow more complete comparisons with previously published data.

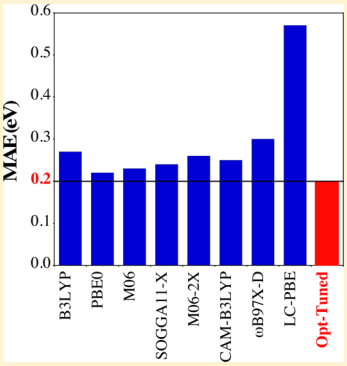

1. INTRODUCTION

In density functional theory (DFT), the adequate choice of an approximate exchange-correlation functional (XCF) is often key to obtaining chemically accurate ground-state (GS) properties. The XCF selection becomes of utmost importance in time-dependent density functional theory (TD-DFT)[1,2] linear and higher-order response methods that allow accessing differences between GS and excited-state (ES) energies, transition moments, and other properties. Indeed, both the ES energies and structures computed with TD-DFT depend not only quantitatively but also qualitatively on the XCF.[3−5] For most chemical applications, it is well-recognized that "pure" XCFs, i.e. XCFs of the classes that do not include a portion of exact exchange, tend to yield poor results. Therefore, the main challenge is to select the most suited hybrid XCF for a given ES problem. This question gave rise to numerous TD-DFT benchmarks, a topic that has been recently reviewed by one of us.[5]

The popularity of TD-DFT benchmarks can be explained both by the interest in developing theoretical methods able to accurately predict ES features in order to assist the development of several technological applications and by the difficulty to define a rigorous and well-accepted protocol for TD-DFT benchmarks. Indeed, if most TD-DFT applications rely on the vertical approximation to obtain transition energies, the vertical TD-DFT data cannot be straightforwardly compared to experiment. To obtain meaningful comparisons, a useful approach is to determine 0−0 energies. This task involves substantial computational efforts, as the curvature of the ES potential energy surface should be determined.[5−7] The computed 0−0 energies can be compared to the crossover of the experimental absorption and emission curves (AFCP: absorption/fluorescence crossing point) for large molecules or to experimental 0−0 energies for smaller compounds.

To our knowledge, four series of works devoted to general (that is, without focusing on a specific subclass of molecules) 0−0 benchmarks appeared so far: two for gas phase molecules and two for solvated dyes. In the first, Furche and co-workers used a database of 109 ES of small molecules in gas-phase and tested several functionals, namely LSDA, PBE, BP86, TPSS, TPSSh, B3LYP, and PBE0.[8,9] To lighten the computational effort, they used B3LYP zero-point vibrational energies (ZPVE) for all cases. Among the tested XCFs, B3LYP emerged as the most accurate, with a mean absolute deviation (MAE) with respect to experiment of 0.21 eV.[8] Hättig and collaborators proposed a 66 ES set containing highly accurate gas phase references, and they reported a similar performance of B3LYP (MAE of 0.19 eV).[10] Grimme and co-workers performed a series of benchmark calculations[7,11,12] with a focus on "real-life" solvated molecules. In their more recent contribution, they considered 12 large dyes and applied successive corrections (solvent, vibration, and structural relaxation) to allow calculations with a large variety of XCFs.[12] They obtained a

Received: January 28, 2014
Published: February 25, 2014

   dx.doi.org/10.1021/ct5000617 | J. Chem. Theory Comput. 2014, 10, 1677−1685

Scheme 1. Representation of the Set of Molecules Investigated in this Work[a]

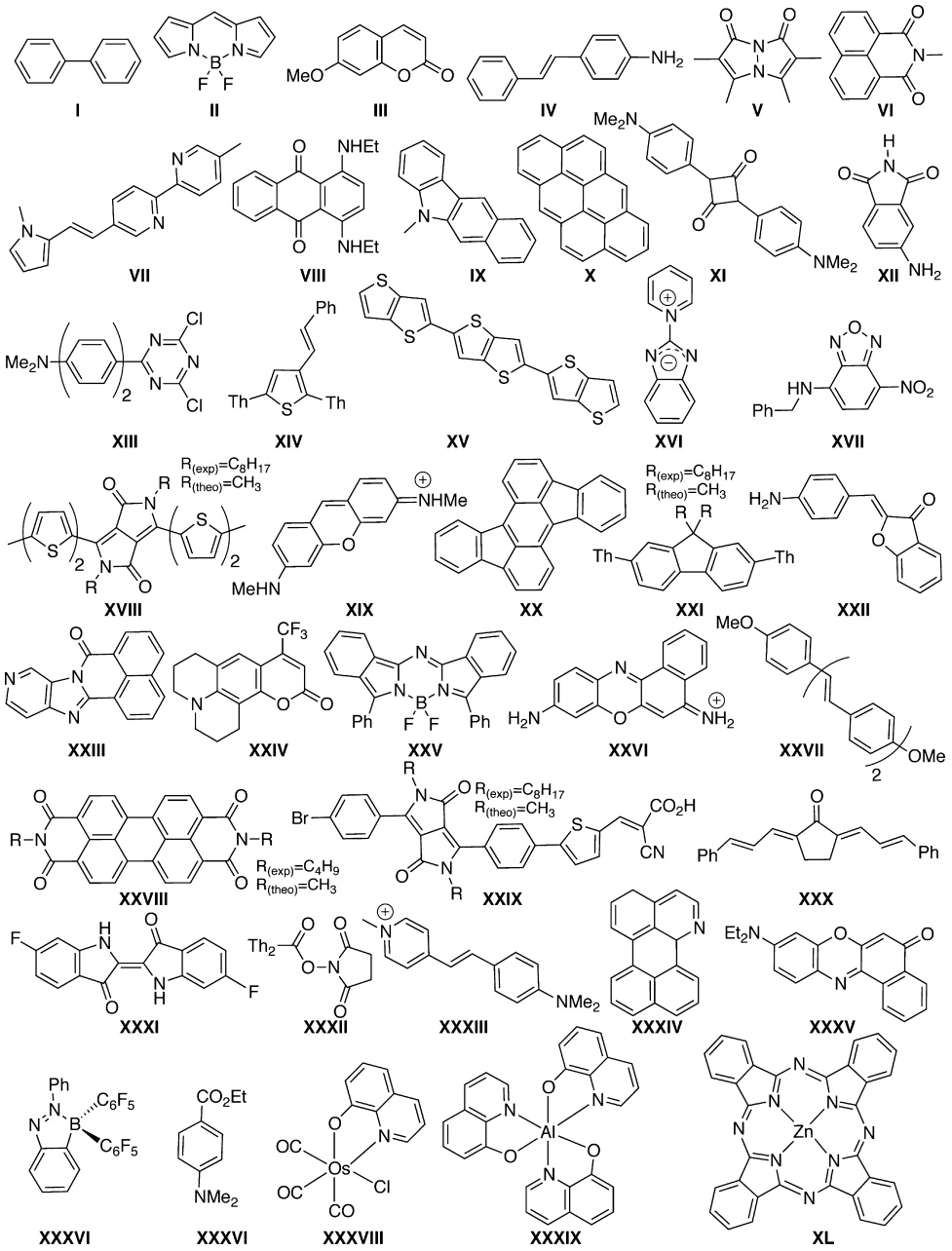

[a]Ph and Th stand for phenyl and thienyl, respectively.

MAE of 0.31 eV for B3LYP, but it could be reduced to 0.19 eV with BMK, 0.18 eV with CAM-B3LYP, and as low as 0.16 eV with the B2GPPLYP double hybrid.[12] In our latest work, we considered 40 medium and large fluorophores in solution (see Scheme 1) and applied as few simplifications as possible (e.g., the ZPVE corrections have been systematically computed for each XCF, a refined environmental model was used, and so forth).[13] With this protocol, we obtained MAEs rather uniform for the tested XCFs, e.g., 0.27 eV with B3LYP, 0.25 eV for CAM-B3LYP, and 0.26 eV with M06-2X. However, only the most promising class of functionals for TD-DFT response calculations, viz., hybrid functionals with range-separated exchange (RSE) or global hybrids including a large share of exact exchange, produced high correlation coefficients (R) between theoretical and experimental data. As one can notice from these four sets of molecules, the reported errors tend to increase for larger compounds. Evidently there remains room for improvements, despite the huge efforts already made in the TD-DFT field.

For this work, we used the set of molecules shown in Scheme 1 in order to assess the usefulness of *optimally tuned* RSE hybrid functionals in the framework of calculations of the 0−0 energies, a task not conducted so far. The optimal tuning approach[14−16] is based on the knowledge that in exact Kohn−Sham (KS) and generalized KS theory, the energy of the highest occupied molecular orbital (HOMO), $\varepsilon_H(N)$, for an N-electron system should be exactly $-\mathrm{IP}(N)$, where IP is the vertical ionization potential calculated with a given functional as the energy difference $E(N-1) - E(N)$. With approximate functionals, differences between $\varepsilon_H(N)$ and $-\mathrm{IP}(N)$ can be very

dx.doi.org/10.1021/ct5000617 | J. Chem. Theory Comput. 2014, 10, 1677−1685

Table 1. Comparison between Theoretical and Experimental AFCP Values (eV)[a]

molecule	solvent	opt γ	LC-PBE*	SOGGA11-X	ωB97X-D	exp	ref
I	cyclohexane	0.234	4.480	4.401	4.500	4.56	49
II	methanol	0.238	2.957	3.043	3.008	2.48	63
III	water	0.251	3.900	3.993	3.986	3.46	46
IV	hexane	0.218	3.411	3.463	3.566	3.50	50
V	ethanol	0.242	3.149	3.352	3.328	2.98	44
VI	dioxane	0.239	3.655	3.654	3.717	3.53	60
VII	benzene	0.201	3.058	3.029	3.189	2.92	68
VIII	cyclohexane	0.202	2.062	2.228	2.268	1.89	70
IX	ethanol	0.209	3.189	3.292	3.411	3.10	43
X	benzene	0.211	2.800	2.812	2.909	2.85	43
XI	dichloromethane	0.182	2.027	2.490	2.442	1.95	49
XII	2-methyl-butane	0.262	3.430	3.544	3.553	3.18	66
XIII	cyclohexane	0.197	3.033	2.961	3.272	2.76	64
XIV	cyclohexane	0.180	2.894	2.983	3.143	3.11	58
XV	dichloromethane	0.180	2.800	2.787	2.947	2.85	67
XVI	toluene	0.245	2.630	2.258	2.686	2.30	71
XVII	ethanol	0.231	2.944	3.032	3.053	2.53	49
XVIII	dichloromethane	0.159	1.995	2.072	2.166	1.95	72
XIX	ethanol	0.212	2.868	3.008	3.020	2.18	43
XX	benzene	0.180	2.188	2.276	2.398	2.29	43
XXI	chloroform	0.188	3.285	3.248	3.448	3.29	54
XXII	ethyl acetate	0.219	3.021	3.074	3.197	2.66	73
XXIII	acetontrile	0.213	3.204	3.223	3.376	2.99	74
XXIV	2-methylbutane	0.215	3.154	3.293	3.380	2.98	51
XXV	chloroform	0.163	1.888	1.971	2.003	1.71	62
XXVI	ethanol	0.207	2.509	2.622	2.629	2.02	45
XXVII	chloroform	0.183	2.977	2.997	3.161	3.15	53
XXVIII	dimethylformamide	0.198	2.351	2.389	2.508	2.33	76
XXIX	dichloromethane	0.171	2.136	2.198	2.504	2.24	75
XXX	ethanol	0.182	2.672	2.798	2.967	2.65	55
XXXI	dioxane	0.207	2.261	2.477	2.525	2.12	57
XXXII	dichloromethane	0.219	3.372	3.407	3.439	3.25	59
XXXIII	water	0.203	2.771	2.830	2.943	2.40	65
XXXIV	acetontrile	0.213	2.802	2.780	2.908	2.76	69
XXXV	carbontetrachloride	0.194	2.533	2.696	2.746	2.28	48
XXXVI	hexane	0.192	2.475	2.919	2.968	2.72	61
XXXVII	ethanol	0.234	4.127	4.271	4.295	3.88	49
XXXVIII	toluene	0.211	2.591	2.751	2.824	2.64	56
XXXIX	dimethylformamide	0.180	2.433	2.755	2.844	2.76	52
XL	toluene	0.157	1.916	1.959	1.879	1.83	47

[a]The optimal range separation parameter γ (a.u.) used in the LC-PBE* calculation, as well as the solvent, are also reported for each structure. Molecules are depicted in Scheme 1.

large.[17] Optimal tuning implies a nonempirical determination of a system-specific range-separation parameter γ in an RSE functional and, optionally, other parameters,[18,19] such that $\varepsilon_H(N) = -IP(N)$ is satisfied to the best possible degree. The IP tuning may be carried out to find an optimal γ for the N and $N + 1$ electron species simultaneously in order to give simple physical interpretations to the energies of the HOMO and the energy $\varepsilon_L(N)$ of the lowest unoccupied MO (LUMO), namely to the best possible degree

$$IP(N) = -\varepsilon_H(N)$$

$$EA(N) = -\varepsilon_L(N)$$

where $EA(N) = IP(N + 1)$ is the electron affinity of the N-electron species. There is now a rapidly increasing number of studies showing that this nonempirical tuning may lead to vastly improved electronic spectra as well as other response properties obtained from TD-DFT, in particular in cases where the DFT delocalization error (DE)[20] leads to poor performance and/or for charge-transfer excitations (CT). There is an underlying connection of the CT problem with the DE and the absence or presence of curvature in the energy as a function of noninteger N that was discussed recently.[21] Solid evidence has been obtained that tuned RSE functionals typically afford a small DE[16,19,22−26] and that they may improve optical gaps.[27,28] As the DE is a potentially serious source of error in calculations of photophysical properties of extended π-chromophores, it is important to investigate whether optimal tuning of the RSE form of a standard functional is able to improve the 0−0 energies. Moreover, it is vital that the optimal tuning does not lead to an overall deterioration of the MAEs and the correlation coefficients or to gross outliers.

It is shown herein that optimal tuning indeed improves the MAEs of a diverse set of chromophores without obvious

dx.doi.org/10.1021/ct5000617 | J. Chem. Theory Comput. 2014, 10, 1677−1685

negative side effects. In particular, the obtained MAE with the tuned RSE hybrid is smaller than with PBE0, M06-2X, or ωB97X-D, three of the most efficient functionals for excited-state energies.

2. METHODOLOGY

2.1. Finding an Optimal Range-Separation Parameter. The RSE tuning has been carried out based on the following separation of the inverse interelectronic distance into a long-range and a short-range part[29]

$$\frac{1}{r_{12}} = \frac{\alpha + \beta \mathrm{erf}(\gamma r_{12})}{r_{12}} + \frac{1 - [\alpha + \beta \mathrm{erf}(\gamma r_{12})]}{r_{12}} \quad (1)$$

in conjunction with the Perdew−Burke−Ernzerhof (PBE)[30] exchange-correlation functional. The dimensionless parameter α and the sum $\alpha + \beta$ correspond to the fraction of exact exchange in the RSE kernel at short and long interelectronic distances r_{12}, respectively. For each molecule from the set in Scheme 1, a tuned form of the long-range corrected PBE functional, LC-PBE ($\alpha = 0$, $\beta = 1$), has been obtained by minimizing J^2 of eq 2

$$J^2 = \sum_{i=0}^{1} [\varepsilon_H(N + i) + \mathrm{IP}(N + i)]^2 \quad (2)$$

with respect to the range-separation parameter γ. Through interpolation from a grid of γ points, the optimal γ has an estimated precision of 0.01 or better, with J^2 at the minimum being practically zero.

The ionization potential IP for a given γ is calculated from the difference of total energies, i.e. $\mathrm{IP}(N) = E(N - 1) - E(N)$, as already mentioned. For additional technical details regarding the tuning procedure and further references see refs 22 and 26. Due to the size of the chromophores and the already very promising performance of the γ-tuned functional, referred to as LC-PBE* in the following, we decided to forego a more demanding "two-dimensional" tuning whereby γ and $\alpha = 1 - \beta$ are found to minimize eq 2 and eliminate a residual DFT delocalization error.[18,19] Additional results will be published subsequently.

2.2. Computing the AFCP. The method used to obtain the AFCP energies was fully described in a previous contribution.[13] For brevity, we only summarize the procedure here using a compact notation. The interested reader will find extensive details and justifications in the cited earlier work. In the following eq and neq stand, respectively, for the equilibrium and nonequilibrium limits of the selected environmental model, that are adequate for slow and fast electronic phenomena, respectively; whereas, cLR[31] and LR[32,33] respectively indicate the corrected linear-response and the linear-response approximations for the solvent approach (see below). SBS and LBS denotes the small and large atomic basis sets used in the calculations. The best estimates of the AFCP energies reported in Table 1 are obtained as

$$E^{\mathrm{AFCP}} = E_{\mathrm{SBS}}^{\mathrm{adia}}(\mathrm{cLR, eq}) + [E_{\mathrm{LBS}}^{\mathrm{adia}}(\mathrm{LR, eq}) - E_{\mathrm{SBS}}^{\mathrm{adia}}(\mathrm{LR, eq})] + \Delta E_{\mathrm{SBS}}^{\mathrm{ZPVE}}(\mathrm{LR, eq}) + \Delta E_{\mathrm{SBS}}^{\mathrm{neq/eq}}(\mathrm{cLR}) \quad (3)$$

where the adiabatic energies are determined as the energy difference between the two states at their respective optimal geometries (denoted R)

$$E_{\mathrm{BS}}^{\mathrm{adia}}(X, \mathrm{eq}) = E_{\mathrm{BS}}^{\mathrm{ES}}(R^{\mathrm{ES}}, X, \mathrm{eq}) - E_{\mathrm{BS}}^{\mathrm{GS}}(R^{\mathrm{GS}}, \mathrm{eq}) \quad (4)$$

the correction for the ZPVE difference between the two states is simply the following:

$$\Delta E_{\mathrm{BS}}^{\mathrm{ZPVE}}(\mathrm{LR, eq}) = E_{\mathrm{BS}}^{\mathrm{ZPVE}}(R^{\mathrm{ES}}, \mathrm{LR, eq}) - E_{\mathrm{BS}}^{\mathrm{ZPVE}}(R^{\mathrm{GS}}, \mathrm{eq}) \quad (5)$$

The last term of eq 3 that corresponds to the nonequilibrium corrections necessary to transform the equilibrium 0−0 energies in nonequilibrium AFCP energies can be obtained from the difference between neq and eq vertical absorption and fluorescence energies calculated as

$$\Delta E_{\mathrm{BS}}^{\mathrm{neq/eq}}(\mathrm{cLR}) = \frac{1}{2}[\Delta E_{\mathrm{BS}}^{\mathrm{abso-neq/eq}}(\mathrm{cLR}) + \Delta E_{\mathrm{BS}}^{\mathrm{fluo-neq/es}}(\mathrm{cLR})] \quad (6)$$

$$\Delta E_{\mathrm{BS}}^{\mathrm{abso-neq/eq}}(\mathrm{cLR}) = E_{\mathrm{BS}}^{\mathrm{ES}}(R^{\mathrm{GS}}, \mathrm{cLR, neq}) - E_{\mathrm{BS}}^{\mathrm{ES}}(R^{\mathrm{GS}}, \mathrm{cLR, eq}) \quad (7)$$

$$\Delta E_{\mathrm{BS}}^{\mathrm{fluo-neq/eq}}(\mathrm{cLR}) = E_{\mathrm{BS}}^{\mathrm{GS}}(R^{\mathrm{ES}}, \mathrm{eq}) - E_{\mathrm{BS}}^{\mathrm{GS}}(R^{\mathrm{ES}}, \mathrm{cLR, neq}) \quad (8)$$

3. COMPUTATIONAL DETAILS

Except for the RSE tuning, all calculations have been performed with the latest commercial version of the Gaussian package.[34] We have improved upon the default thresholds for both the geometry optimization (tight, corresponding to a residual rms force smaller than 10^{-5} a.u.) and energy convergence (at least 10^{-9} a.u.), as well as used better than the default DFT integration grids: a grid with 99 radial shells and 590 angular points per shell (*ultrafine* grid in Gaussian09) was systematically used but for the coupled-perturbed Kohn−Sham part that relied on a slightly smaller grid (*fine* grid corresponding to 75 radial shells and 302 angular points per shell). These changes have been made to ensure numerically stable and accurate calculations while retaining computational efficiency. The GS and ES geometries have been optimized with DFT and TD-DFT, starting from the optimal CAM-B3LYP structures available in the Supporting Information of ref 13. Next, vibrational frequencies have been determined for each state so that, of course, all structures presented below correspond to true minima of the potential energy surface (absence of imaginary frequencies). When possible, point group symmetry has been used to reduce the computational effort and the same point group has been systematically used for both states (lowering the symmetry of the states presenting the higher point group when necessary). The applied SBS and LBS (see above) were 6-31+G(d) and 6-311++G(2df,2p), respectively. As for the tuning procedure, LANL2DZ was used for the metallic atoms. These choices guarantee convergence of the data: using even larger atomic basis sets leads to completely trifling variations for the cases of interest.[13] Solvent effects have been systematically accounted for by using the polarizable continuum model (PCM).[35] For both optimizations and frequency calculations, we have applied the only available model, that is the linear-response approach.[32,33] The (single-point) energies were computed with the corrected linear-response model that provides more accurate estimations of the polarization of the cavity at the ES, thanks to the explicit calculation of the ES density.[31] In addition to the optimally tuned XCF, LC-PBE*, we have tested two additional

dx.doi.org/10.1021/ct5000617 | J. Chem. Theory Comput. 2014, 10, 1677−1685

functionals, namely Truhlar's SOGGA11-X[36] and Head-Gordon's ωB97X-D.[37] These choices were made to complement our previous investigations: on the one hand, the global SOGGA11-X hybrid contains 40.15% of exact exchange whereas the previously tested global hybrid XCF for this set of molecules contained either 20−27% (B3LYP, PBE0 and M06) or 54% (M06-2X) of exact exchange, and, on the other hand, ωB97X-D is a range-separated XCF with a small RSE parameter (0.2 au) and a correct asymptotic behavior, that has recently been considered as one of the most efficient XCF for ES properties.[38]

The calculations to determine the range-separation parameters to arrive at optimally tuned RSE functionals were performed with a developers' version of NWChem[39,40] using the 6-31+G(d) basis set for all atoms, except for zinc and osmium where the LANL2DZ basis set and matching effective core potentials were used.[41,42] Single-point energy calculations with the PBE functional were carried out for the anion, cation, and neutral systems, and the resulting orbitals were used as initial guesses for the RSE calculations with LC-PBE with varying γ values. In all of the tuning calculations we used an "extra fine" numerical integration grid together with an energy convergence of 10^{-8} a.u.. The tuning step used the CAM-B3LYP structures from ref 13 as it is safe to assume that the optimal range-separation parameters are not strongly dependent on the optimization level. In order to test this assumption, for chromophores **I**−**V** the optimal ground state γ were redetermined for the excited state structures optimized with LC-PBE*. The changes with respect to the optimal ground state RSE parameters were 0.08 au or less. The AFCPs calculated with tuned γ values for the excited state geometry changed by 0.014 eV or less relative to the calculations with the parameters determined for the ground state structures. These data are available in the Supporting Information (SI).

4. RESULTS

Table 1 lists the solvent, the optimal γ values, the AFCP energies computed with the three functionals as well as the experimental energies extracted from several works.[43−76]

The γ values collected in Table 1 are between 0.157 and 0.262 a.u., that is, they cover a relatively small range of possible values. For instance, the default γ value for LC-PBE in Gaussian09 is 0.470 a.u.;[77] whereas the popular CAM-B3LYP hybrid uses 0.330 a.u.[29] The tuning data show that these default values for general parametrizations of popular RSE functionals are significantly too large for the dyes under consideration in this work. For the tested dyes, the smallest γ value is obtained for the largest dye, the phthalocyanine **XL**, whereas the largest values is reached for **XII**, one of the most compact of the molecules considered. In general one notices that the larger the π conjugated path in the dye the smaller the optimal γ value. The correlation coefficient, R, between HOMO−LUMO gaps and the optimal γ is 0.80 (see the SI for a plot). As γ has the dimension of an inverse distance, $1/\gamma$ may also be associated with an effective conjugation length in the chromophore which may increase toward a limiting value for a given class of chromophore as the size of the π system increases. This behavior is consistent with a number of previous studies.[22,27,78,79]

As can be seen in Table 1, the optimally tuned XCF generally provides accurate AFCP energies, despite the diversity of the structures selected. Compared to all other tested XCF, the most notable improvement brought by LC-PBE* is found for the squaraine **XI**, a quadrupolar molecule with a push−pull−push nature. Nevertheless, let us focus at this stage on the most problematic cases in order to understand the reasons for the outliers. The two largest theory−experiment deviations obtained with LC-PBE* correspond to molecules **XIX** and **XXVI** for which theory strongly overestimates the experimental reference, by 0.68 and 0.49 eV, respectively, despite the optimal tuning (SOGGA11-X and ωB97X-D yield even less accurate estimates). We note that these deviations are slightly smaller than the one obtained with M06-2X but exceed their B3LYP counterparts,[13] which can be explained in terms of two aspects. First, both compounds are cyanines and it is well-known that TD-DFT, irrespective of the selected XCF, overshoots the transition energies of such dyes, a systematic effect mitigated, but not eliminated, by the use of the most modern XCFs.[26,80−82] Second, these two charged dyes are solvated in a protic solvent (ethanol) that could obviously interact specifically with both the amine groups and lone pairs of the chromophore. In other words, the use of a continuum model for modeling the environment might not be ideal for these cases. Other molecules for which large deviations from experiment are found with LC-PBE* suffer from one of these two aspects, e.g., **III** is solvated in water, **XVII** is solvated in ethanol, and **II** is a BODIPY dye, that can be viewed as a constrained cyanine. For both **II** and **III**, the accuracy provided by LC-PBE* is in the line of CAM-B3LYP or M06-2X[13] and slightly outperforms both SOGGA11-X and ωB97X-D. For **XVII**, the 0.42 eV overestimation of LC-PBE* is again similar to CAM-B3LYP, though in that case B3LYP provides much more accurate data, a quite surprising fact for a compound with a significant push−pull character. The strongest underestimation of the AFCP with LC-PBE* is found for **XXXIX**, but the absolute deviation is smaller than for the molecules discussed above (0.33 eV). In our previous work,[13] we have pointed out that molecule **XIII** undergoes the well-known ES overtwisting problem with functionals not including a large

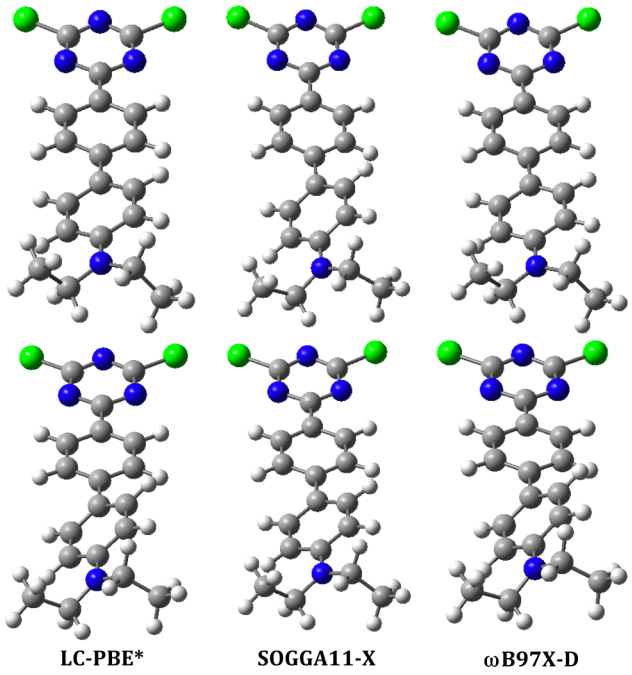

Figure 1. Perspective view of the optimal GS (bottom) and ES (top) geometries computed for molecule **XIII**, using three different XCF (LC-PBE*, SOGGA11-X, and ωB97X-D).

dx.doi.org/10.1021/ct5000617 | J. Chem. Theory Comput. 2014, 10, 1677−1685

Table 2. Statistical Analysis Obtained from the Comparison of the Theoretical and the Experimental AFCP Listed in Table 1[a]

method	MSE	MAE	RMS	SD	*R*	max(+)	max(−)
PBE0	0.03	0.22	0.28	0.17	0.89	0.79	−0.64
SOGGA11-X	−0.21	0.24	0.31	0.20	0.92	0.16	−0.83
M06-2X	−0.25	0.26	0.31	0.18	0.95	0.08	−0.77
ωB97X-D	−0.30	0.30	0.36	0.19	0.94	0.06	−0.84
LC-PBE*	−0.12	0.20	0.25	0.15	0.93	0.33	−0.68
LC-PBE	−0.56	0.57	0.60	0.20	0.94	0.18	−1.10

[a]All values are in electronvolts. The PBE0, M06-2X, and LC-PBE (γ = 0.47 a.u.) data have been taken from ref 13.

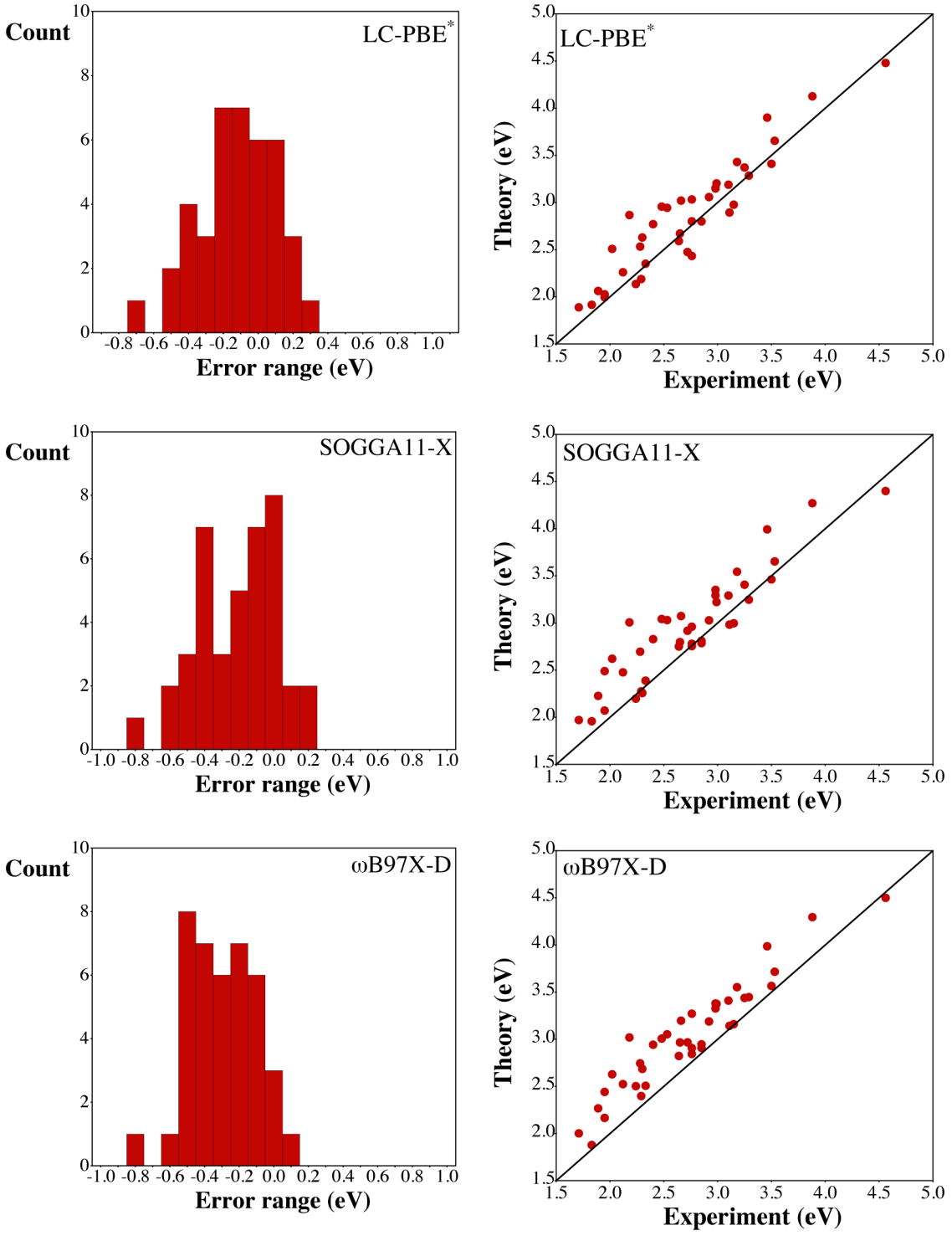

Figure 2. Histograms of the errors (left) and theory−experiment comparisons (right) obtained for three XCFs.

dx.doi.org/10.1021/ct5000617 | J. Chem. Theory Comput. 2014, 10, 1677−1685

fraction of exact exchange. E.g., with B3LYP the aromatic rings become perpendicular when optimizing the ES geometry, an artifact related to the localization of the frontier orbitals on two noninteracting parts of the molecule.[4,83,84] All three XCF tested here pass this test and provide a qualitatively sound ES structure (see Figure 1), with large oscillator strengths ($f > 1$) in all cases. Another challenging molecule is **XXXVI**. The three XCFs considered in the present work provide relatively similar and sizable f for the (vertical) absorption to the first ES, 0.39, 0.47, and 0.46 for LC-PBE*, SOGGA11-X, and ωB97X-D, respectively. However, the vertical emissions computed on the ES structure give vastly different oscillator strengths: 0.05, 0.52, and 0.51 for the three functionals, respectively. This strong decrease of f between the GS and ES for LC-PBE* was also noted for standard global hybrids, e.g., B3LYP, but is likely to be unphysical, as experimentally the related quantum yield of fluorescence is large.[61] This decrease of f is accompanied with a larger Stokes shift for LC-PBE* (7940 cm^{-1} using the vertical cLR,neq approximation) than for SOGGA11-X (5726 cm^{-1}) and ωB97X-D (6154 cm^{-1}), the two latter being in better match with experiment (6026 cm^{-1}),[61] hinting that LC-PBE* does not systematically improve the description provided by other XCFs.

In Table 2, we report the results of a statistical analysis—mean signed error (MSE), mean absolute error (MAE), root-mean-square deviation (RMS), standard deviation (SD), and linear correlation coefficient (R) as well as the maximal and the minimal deviations—obtained by comparing the experimental and theoretical values listed in Table 1. Figure 2 provides a graphical representation of the error patterns obtained for three of the six hybrid functionals. The MSE is slightly negative for LC-PBE* (−0.12 eV) indicating that this functional tend to overestimate (on average) the experimental 0−0 excitation energies, but this effect is significantly stronger for both SOGGA11-X (−0.21 eV) and ωB97X-D (−0.30 eV). The MAE obtained with the latter functional is rather large (0.30 eV), and it can be seen in Figure 2 that this range-separated hybrid functional systematically overestimates the experimental points, albeit there is one exception. SOGGA11-X statistical parameters are in between PBE0 and M06-2X, indicating that the fraction of exact exchange included in the XCF is indeed the key parameter for global hybrids. The smallest MAE, RMS, and SD are reached with LC-PBE*, which slightly outperforms PBE0 and M06 and represents the most efficient XCF for these three parameters up to now.[13] Moreover, this success of LC-PBE* comes with a rather large R (0.93 compared to 0.89 for both PBE0 and M06) as some of the most notable inconsistencies of standard global hybrids are cured with LC-PBE*. From Figure 2, one also notices that the error pattern present a nearly Gaussian shape for LC-PBE*; whereas, it is significantly less symmetric for the two other functionals. Nevertheless, we note that M06-2X and ωB97X-D still provide slightly larger R than LC-PBE*. For the record, we have performed a statistical analysis of the optimally tuned results removing all cases in protic solvents (methanol, ethanol and water), and, for the 31 remaining points, we obtained a MAE of 0.16 eV and a SD of 0.11 eV: the values reported above are probably upper limits, but this statement applies to all XCFs.

5. CONCLUSIONS AND OUTLOOK

We have evaluated the efficiency of an optimally tuned hybrid functional with range-separated exchange in reproducing the experimental 0−0 energies of a large set of solvated molecules. The use of LC-PBE* reduced the deviations with respect to experiment to a MAE of 0.20 eV, a rather small value for a set of dyes containing several challenging cases. The two other tested functionals, SOGGA11-X and ωB97X-D, produced larger deviations (0.24 and 0.30 eV, respectively). It is also remarkable that the LC-PBE* standard deviation (0.15 eV) is small and the correlation coefficient with experimental data is large (0.93), though it is slightly smaller than the one obtained with M06-2X (0.95) or ωB97X-D (0.94). In short, optimally tuned range-separated hybrids provide the best of the two worlds: large consistency (typical of hybrid functionals containing a large share of exact exchange) and small absolute deviations (typical of hybrid functionals with a small exact exchange ratio).

Additional improvements may be achieved by finding an optimal combination of the RSE parameter and a nonzero fraction of exact exchange at short interelectronic separation (parameter α in eq 1) via two-dimensional tuning.[18]

■ ASSOCIATED CONTENT

Supporting Information

Raw data: absorption, fluorescence, and adiabatic energies, as well as ZPVE difference for all investigated cases. Values of γ (and AFCP values) determined for excited-state structures. Correlation plot between H−L gap and optimal γ values. This material is available free of charge via the Internet at http://pubs.acs.org/.

■ AUTHOR INFORMATION

Corresponding Authors

*E-mail: Denis.Jacquemin@univ-nantes.fr.
*E-mail: jochena@buffalo.edu.

Notes

The authors declare no competing financial interest.

■ ACKNOWLEDGMENTS

D.J. acknowledges the European Research Council (ERC) and the *Région des Pays de la Loire* for financial support in the framework of a Starting Grant (Marches-278845) and a *recrutement sur poste stratégique*, respectively. J.A. and B.M. are grateful for financial support of this research by the National Science Foundation, grants CHE-0952253 and CHE-1265833. This research used resources of (1) the GENCI-CINES/IDRIS, (2) CCIPL (*Centre de Calcul Intensif des Pays de Loire*), (3) a local Troy cluster, and (4) the Center for Computational Research at SUNY Buffalo. The authors are indebted to the COST program CODECS and its members for support and many helpful discussions, respectively.

■ REFERENCES

(1) Runge, E.; Gross, E. K. U. *Phys. Rev. Lett.* **1984**, *52*, 997−1000.
(2) Casida, M. E. In *Time-Dependent Density-Functional Response Theory for Molecules*; Chong, D. P., Ed.; World Scientific: Singapore, 1995; Vol. *1*, pp 155−192.
(3) Dreuw, A.; Head-Gordon, M. *J. Am. Chem. Soc.* **2004**, *126*, 4007−4016.
(4) Wiggins, P.; Gareth Williams, J. A.; Tozer, D. J. *J. Chem. Phys.* **2009**, *131*, 091101.
(5) Laurent, A. D.; Jacquemin, D. *Int. J. Quantum Chem.* **2013**, *113*, 2019−2039.
(6) Furche, F.; Ahlrichs, R. *J. Chem. Phys.* **2002**, *117*, 7433−7447.
(7) Dierksen, M.; Grimme, S. *J. Phys. Chem. A* **2004**, *108*, 10225−10237.

(8) Send, R.; Kühn, M.; Furche, F. *J. Chem. Theory Comput.* **2011**, *7*, 2376−2386.
(9) Bates, J. E. E.; Furche, F. *J. Chem. Phys.* **2012**, *137*, 164105.
(10) Winter, N. O. C.; Graf, N. K.; Leutwyler, S.; Hättig, C. *Phys. Chem. Chem. Phys.* **2013**, *15*, 6623−6630.
(11) Goerigk, L.; Moellmann, J.; Grimme, S. *Phys. Chem. Chem. Phys.* **2009**, *11*, 4611−4620.
(12) Goerigk, L.; Grimme, S. *J. Chem. Phys.* **2010**, *132*, 184103.
(13) Jacquemin, D.; Planchat, A.; Adamo, C.; Mennucci, B. *J. Chem. Theory Comput.* **2012**, *8*, 2359−2372.
(14) Baer, R.; Livshits, E.; Salzner, U. *Annu. Rev. Phys. Chem.* **2010**, *61*, 85−109.
(15) Stein, T.; Eisenberg, H.; Kronik, L.; Baer, R. *Phys. Rev. Lett.* **2010**, *105*, 266802−4.
(16) Kronik, L.; Stein, T.; Refaely-Ambrason, S.; Baer, R. *J. Chem. Theory Comput.* **2012**, *8*, 1515−1531.
(17) Gritsenko, O. V.; Baerends, E. J. *J. Chem. Phys.* **2004**, *121*, 655−660.
(18) Srebro, M.; Autschbach, J. *J. Phys. Chem. Lett.* **2012**, *3*, 576−581.
(19) Refaely-Abramson, S.; Sharifzadeh, S.; Govind, N.; Autschbach, J.; Neaton, J. B.; Baer, R.; Kronik, L. *Phys. Rev. Lett.* **2012**, *109*, 226405−5.
(20) Cohen, A. J.; Mori-Sánchez, P.; Yang, W. *Science* **2008**, *321*, 792−794.
(21) Stein, T.; Autschbach, J.; Govind, N.; Kronik, L.; Baer, R. *J. Phys. Chem. Lett.* **2012**, *3*, 3740−3744.
(22) Sun, H.; Autschbach, J. *ChemPhysChem* **2013**, *14*, 2450−2461.
(23) Moore, B., II; Autschbach, J. *ChemistryOpen* **2012**, *1*, 184−194.
(24) Moore, B., II; Srebro, M.; Autschbach, J. *J. Chem. Theory Comput.* **2012**, *8*, 4336−4346.
(25) Gledhill, J. D.; Peach, M. J. G.; Tozer, D. J. *J. Chem. Theory Comput.* **2013**, *9*, 4414−4420.
(26) Moore, B., II; Autschbach, J. *J. Chem. Theory Comput.* **2013**, *9*, 4991−5003.
(27) Refaely-Ambrason, S.; Baer, R.; Kronik, L. *Phys. Rev. B* **2011**, *84*, 075144.
(28) Sun, H.; Autschbach, J. *J. Chem. Theory Comput.* **2014**, DOI: 10.1021/ct4009975.
(29) Yanai, T.; Tew, D. P.; Handy, N. C. *Chem. Phys. Lett.* **2004**, *393*, 51−56.
(30) Perdew, J. P.; Burke, K.; Ernzerhof, M. *Phys. Rev. Lett.* **1996**, *77*, 3865−3868.
(31) Caricato, M.; Mennucci, B.; Tomasi, J.; Ingrosso, F.; Cammi, R.; Corni, S.; Scalmani, G. *J. Chem. Phys.* **2006**, *124*, 124520.
(32) Cammi, R.; Mennucci, B. *J. Chem. Phys.* **1999**, *110*, 9877−9886.
(33) Cossi, M.; Barone, V. *J. Chem. Phys.* **2001**, *115*, 4708−4717.
(34) Frisch, M. J.; Trucks, G. W.; Schlegel, H. B.; Scuseria, G. E.; Robb, M. A.; Cheeseman, J. R.; Scalmani, G.; Barone, V.; Mennucci, B.; Petersson, G. A.; Nakatsuji, H.; Caricato, M.; Li, X.; Hratchian, H. P.; Izmaylov, A. F.; Bloino, J.; Zheng, G.; Sonnenberg, J. L.; Hada, M.; Ehara, M.; Toyota, K.; Fukuda, R.; Hasegawa, J.; Ishida, M.; Nakajima, T.; Honda, Y.; Kitao, O.; Nakai, H.; Vreven, T.; Montgomery, J. A., Jr.; Peralta, J. E.; Ogliaro, F.; Bearpark, M.; Heyd, J. J.; Brothers, E.; Kudin, K. N.; Staroverov, V. N.; Kobayashi, R.; Normand, J.; Raghavachari, K.; Rendell, A.; Burant, J. C.; Iyengar, S. S.; Tomasi, J.; Cossi, M.; Rega, N.; Millam, J. M.; Klene, M.; Knox, J. E.; Cross, J. B.; Bakken, V.; Adamo, C.; Jaramillo, J.; Gomperts, R.; Stratmann, R. E.; Yazyev, O.; Austin, A. J.; Cammi, R.; Pomelli, C.; Ochterski, J. W.; Martin, R. L.; Morokuma, K.; Zakrzewski, V. G.; Voth, G. A.; Salvador, P.; Dannenberg, J. J.; Dapprich, S.; Daniels, A. D.; Farkas, O.; Foresman, J. B.; Ortiz, J. V.; Cioslowski, J.; Fox, D. J. *Gaussian 09 Revision D.01*; Gaussian Inc.: Wallingford, CT, 2009.
(35) Tomasi, J.; Mennucci, B.; Cammi, R. *Chem. Rev.* **2005**, *105*, 2999−3094.
(36) Peverati, R.; Truhlar, D. *J. Chem. Phys.* **2011**, *135*, 191102−191102.
(37) Chai, J. D.; Head-Gordon, M. *Phys. Chem. Chem. Phys.* **2008**, *10*, 6615−6620.
(38) Isegawa, M.; Peverati, R.; Truhlar, D. G. *J. Chem. Phys.* **2012**, *137*, 244104.
(39) Valiev, M.; Bylaska, E. J.; Govind, N.; Kowalski, K.; Straatsma, T. P.; Van Dam, H. J. J.; Wang, D.; Nieplocha, J.; Apra, E.; Windus, T. L.; de Jong, W. A. *Comput. Phys. Commun.* **2010**, *181*, 1477−1489.
(40) Bylaska, E. J.; de Jong, W. A.; Govind, N.; Kowalski, K.; Straatsma, T. P.; Valiev, M.; van Dam, J. J.; Wang, D.; Apra, E.; Windus, T. L.; Hammond, J.; Autschbach, J.; Aquino, F.; Nichols, P.; Hirata, S.; Hackler, M. T.; Zhao, Y.; Fan, P.-D.; Harrison, R. J.; Dupuis, M.; Smith, D. M. A.; Glaesemann, K.; Nieplocha, J.; Tipparaju, V.; Krishnan, M.; Vazquez- Mayagoitia, A.; Jensen, L.; Swart, M.; Wu, Q.; Van Voorhis, T.; Auer, A. A.; Nooijen, M.; Crosby, L. D.; Brown, E.; Cisneros, G.; Fann, G. I.; Fruchtl, H.; Garza, J.; Hirao, K.; Kendall, R.; Nichols, J. A.; Tsemekhman, K.; Wolinski, K.; Anchell, J.; Bernholdt, D.; Borowski, P.; Clark, T.; Clerc, D.; Dachsel, H.; Deegan, M.; Dyall, K.; Elwood, D.; Glendening, E.; Gutowski, M.; Hess, A.; Jaffe, J.; Johnson, B.; Ju, J.; Kobayashi, R.; Kutteh, R.; Lin, Z.; Littlefield, R.; Long, X.; Meng, B.; Nakajima, T.; Niu, S.; Pollack, L.; Rosing, M.; Sandrone, G.; Stave, M.; Taylor, H.; Thomas, G.; van Lenthe, J.; Wong, A.; Zhang, Z. *NWChem, A Computational Chemistry Package for Parallel Computers, Version 6 (2012 developer's version)*; Pacific Northwest National Laboratory: Richland, WA, USA, 2012.
(41) Hay, P. J.; Wadt, W. R. *J. Chem. Phys.* **1985**, *82*, 270.
(42) Hay, P. J.; Wadt, W. R. *J. Chem. Phys.* **1985**, *82*, 284.
(43) Berlman, I. B. *Handbook of fluorescence spectra of aromatic molecules*, 2nd ed.; Academic Press: New York, 1971; p 258.
(44) Pavlopoulos, T. G. *J. Appl. Phys.* **1986**, *60*, 4028−4030.
(45) Kreller, D. I.; Kamat, P. V. *J. Phys. Chem.* **1991**, *95*, 4406−4410.
(46) Heldt, J. R.; Helds, J.; Ston, M.; Diehl, H. A. *Spectrochim. Acta A* **1995**, *51*, 1549−1563.
(47) Bishop, S.; Beeby, A.; Parker, A.; Foley, M.; Phillips, D. *J. Photochem. Photobiol. A: Chem.* **1995**, *90*, 39−44.
(48) Dutta, A. K.; Kamada, K.; Ohta, K. *J. Photochem. Photobiol. A: Chem.* **1996**, *93*, 57−64.
(49) Du, H.; Fuh, R. A.; Li, J.; Corkan, A.; Lindsey, J. S. *Photochem. Photobiol.* **1998**, *68*, 141−142. Spectra available at http://omlc.ogi.edu/spectra/PhotochemCAD/ (accessed April 4, 2013) and http://www.fluorophores.tugraz.at/ (accessed April 4, 2013).
(50) Lewis, F. D.; Kalgutkar, R. S.; Yang, J.-S. *J. Am. Chem. Soc.* **1999**, *121*, 12045−12053.
(51) Mühlpfordt, A.; Schanz, R.; Ernsting, N. P.; Farztdinov, V.; Grimme, S. *Phys. Chem. Chem. Phys.* **1999**, *1*, 3209−3218.
(52) van Veldhoven, E.; Zhang, H.; Glasbeek, M. *J. Phys. Chem. A* **2001**, *105*, 1687−1692.
(53) Ichino, Y.; Ni, J. P.; Ueda, Y.; Wang, D. K. *Synth. Met.* **2001**, *116*, 223−227.
(54) Belletete, M.; Morin, J. F.; Beaupre, S.; Ranger, M.; Leclerc, M.; Durocher, G. *Macromolecules* **2001**, *34*, 2288−2297.
(55) Connors, R. E.; Ucak-Astarlioglu, M. G. *J. Phys. Chem. A* **2003**, *107*, 7684−7691.
(56) Cheng, Y. M.; Yeh, Y. S.; Ho, M. L.; Chou, P. T.; Chen, P. S.; Chi, Y. *Inorg. Chem.* **2005**, *44*, 4594−4603.
(57) Seixas de Melo, J. S.; Rondao, R.; Burrows, H. D.; Melo, M. J.; Navaratman, S.; Edge, R.; Voss, G. *ChemPhysChem* **2006**, *7*, 2303−2311.
(58) Clarke, T. C.; Gordon, K. C.; Kwok, W. M.; Phillips, D. L.; Officer, D. L. *J. Phys. Chem. A* **2006**, *110*, 7696−7702.
(59) Barbarella, G.; Zambianchi, M.; Ventola, A.; Fabiano, E.; Della Sala, F.; Gigli, G.; Anni, M.; Bolognesi, A.; Polito, L.; Naldi, M.; Capobianco, M. *Biooconjugate Chem.* **2006**, *17*, 58−67.
(60) Magalhaes, J. L.; Pereira, R. V.; Triboni, E. R.; Berci Filho, P.; Gehlen, M. H.; Nart, F. C. *J. Photochem. Photobiol. A: Chem.* **2006**, *183*, 165−170.
(61) Yoshino, J.; Kano, N.; Kawashima, T. *Chem. Commun.* **2007**, 559−561.
(62) Donyagina, V.; Shimizu, S.; Kobayashi, N.; Lukyanets, E. A. *Tetrahedron Lett.* **2008**, *48*, 6152−6154.
(63) Tram, K.; Yan, H.; Jenkins, H. A.; Vassiliev, S.; Bruce, D. *Dyes Pigm.* **2009**, *82*, 392−395.

(64) Ma, Y.; Hao, R.; Shao, G.; Wang, Y. *J. Phys. Chem. A* **2009**, *113*, 5066−5072.
(65) Abdel-Halim, S. T.; Awad, M. K. *J. Mol. Struct.* **2009**, *920*, 332−341.
(66) Sajadi, M.; Obernhuber, T.; Kovalenko, S. A.; Mosquera, M.; Dick, B.; Ernsting, N. P. *J. Phys. Chem. A* **2009**, *113*, 44−55.
(67) Henssler, J. T.; Zhang, X.; Matzger, A. J. *J. Org. Chem.* **2009**, *74*, 9112−9119.
(68) Younes, A. H.; Zhang, L.; Clark, R. J.; Zhu, L. *J. Org. Chem.* **2009**, *74*, 8761−8772.
(69) Gryko, D. T.; Piechowska, J.; Galzeowski. *J. Org. Chem.* **2010**, *75*, 1297−1300.
(70) Zakerhamidi, M. S.; Ghanadzadeh, A.; Moghadam, M. *SpectroChim. Acta A* **2011**, *79*, 74−81.
(71) Pawlowska, Z.; Lietard, A.; Aloise, S.; Sliwa, M.; Idrissi, A.; Poizat, O.; Buntinx, G.; Delbaere, S.; Perrier, A.; Maurel, F.; Jacques, F.; Abe, J. *Phys. Chem. Chem. Phys.* **2011**, *13*, 13185−13195.
(72) Bruckstummer, H.; Weissenstein, A.; Bialas, D.; Wurthner, F. *J. Org. Chem.* **2011**, *76*, 2426−2432.
(73) Shanker, N.; Dilek, O.; Mukherjee, T.; McGee, D. W.; Bane, S. L. *J. Fluores.* **2011**, *21*, 2173−2184.
(74) Erten-Ela, S.; Ozcelik, S.; Eren, E. *J. Fluores.* **2011**, *21*, 1565−1573.
(75) Warnan, J.; Favereau, L.; Pellegrin, Y.; Blart, E.; Jacquemin, D.; Odobel, F. *J. Photochem. Photobiol. A: Chem.* **2011**, *226*, 9−15.
(76) Georgiev, N. I.; Sakr, A. R.; Bojinov, V. B. *Dyes Pigm.* **2011**, *91*, 332−339.
(77) Song, J. W.; Hirosawa, T.; Tsuneda, T.; Hirao, K. *J. Chem. Phys.* **2007**, *126*, 154105.
(78) Pansare, V. J.; Hejazi, S.; Faenza, W. J.; Prud'homme, R. K. *Chem. Mater.* **2012**, *24*, 812−827.
(79) Körzdörfer, T.; Sears, J. S.; Sutton, C.; Brédas, J.-L. *J. Chem. Phys.* **2011**, *135*, 204107−6.
(80) Grimme, S.; Neese, F. *J. Chem. Phys.* **2007**, *127*, 154116.
(81) Send, R.; Valsson, O.; Filippi, C. *J. Chem. Theory Comput.* **2011**, *7*, 444−455.
(82) Jacquemin, D.; Zhao, Y.; Valero, R.; Adamo, C.; Ciofini, I.; Truhlar, D. G. *J. Chem. Theory Comput.* **2012**, *8*, 1255−1259.
(83) Guido, C. A.; Mennucci, B.; Jacquemin, D.; Adamo, C. *Phys. Chem. Chem. Phys.* **2010**, *12*, 8016−8023.
(84) Plötner, J.; Tozer, D. J.; Dreuw, A. *J. Chem. Theory Comput.* **2010**, *6*, 2315−2324.